A Low-Cost GPS/Inertial Attitude Heading Reference System (AHRS) for General Aviation Applications

Demoz Gebre-Egziabher, Roger C. Hayward and J. David Powell
Department of Aeronautics and Astronautics, Stanford University

ABSTRACT

An inexpensive Attitude Heading Reference System (AHRS) for General Aviation applications is developed by fusing low cost ($20 - $1000) automotive grade inertial sensors with GPS. The inertial sensor suit consists of three orthogonally mounted solid state rate gyros. GPS is used for attitude determination in a triple antenna ultra short baseline configuration. Acomplementary filter is used to combine the information from the inertial sensors with the attitude information derived from GPS. The inertial sensors provide attitude information at a sufficiently high bandwidth to drive an inexpensive glass- cockpit type display for pilot-in-the-loop control. The low bandwidth GPS attitude is used to calibrate the rate gyro biases on-line. In a series of ground and flight tests, it was shown that the system has an accuracy better than 0.2 degrees in yaw, pitch and roll. Data collected during laboratory testing is used to construct error models for the inertial sensors. Analysis based on these models shows that the system can coast through momentary GPS outages lasting 2 minutes with attitude errors less than 6 degrees. Actual performance observed during ground and flight tests with GPS off was found to be substantially better than that predicted by manufacturer supplied specification sheets. Based on this, it is concluded that off-line calibration combined with GPS based in-flight calibration can dramatically improve the performance of inexpensive automotive grade inertial sensors. Data collected from flight tests indicate that some of the automotive grade inertial sensors (180 deg/hr) can perform near the low end of tactical grade (10 deg/hr) sensors for short periods of time after being calibrated on-line by GPS.

I. INTRODUCTION

An AHRS is used in general aviation applications for pilot-in-the-loop control of aircraft attitude and heading. The information presented by the AHRS in most current general aviation aircraft is generated by mechanical gyros. The mechanical gyros used for indicating pitch and roll attitude consist of a spinning rotor that is mounted on a two axis gimbal. The aircraft vacuum or electrical system provides the power needed to spin the rotors in these gyros. As such, these gyros are susceptible to errors that result from the various mechanical forces that are applied to them during normal flight and some require periodic resets by the pilot. The attitude information is presented on mechanical gages that are an integral part of the gyros themselves and have remained the same for decades. The research reported in this paper is aimed at providing reliable, accurate and *affordable* attitude information to the pilot in general aviation aircraft. This is accomplished by taking advantage of the improved sensor and display technologies available today which entails the use of solid state inertial sensors, computer generated “glass cockpit” type displays and attitude determination based on the Global Positioning System (GPS) carrier wave phase measurements.

Most of the previous work at fusing inertial sensors with GPS for attitude determination [1, 2] involved using inertial sensors that were prohibitively expensive for general aviation applications. An attitude system that used fairly inexpensive rate gyros was evaluated in [3]. The inertial-GPS integration in this case was done “off-line” and the system used a long baseline GPS attitude system. Such a system is difficult to install on a general aviation aircraft because the long baselines would mean installation of the GPS antennas on the wing tips which will necessitate extensive wire runs. An additional problem with such a system is the fact that placing antennas on the wing tip introduces wing flexibility as an additional unknown that must be dealt with in the GPS attitude solution. Currently, there are AHRS that use low cost inertial sensors only and are aimed at the general aviation user [4]. These systems employ the traditional AHRS design approach where three rate gyros are aided by level sensors (accelerometers in [4]) and a fluxgate compass. A novel approach to the problem of presenting attitude information for general aviation applications is taken in [5]. Inertial sensors are not used in this system. Instead, a kinematic model of the airplane along with GPS position and velocity measurements derived from a single GPS antenna are used to generate what is termed “pseudo-attitude.”

In the research described in this paper, the approach taken is that of combining GPS attitude derived from an ultra-short baseline system with automotive grade rate gyros to provide attitude in real-time for pilots in the control loop of an aircraft. Section II describes the inertial sensors used in this research and the characterization of the errors associated with the use of these sensors. Section III describes the GPS attitude algorithm. In Section IV, the filter equations used in blending the inertial and GPS attitude solutions will be described. In Section V, flight test data and results are presented. Section VI provides concluding remarks and a summary.

II. INERTIAL SENSORS

The inertial sensors used in this research are of a quality that is labeled as "automotive grade." This term is used to describe these sensors because their primary application is in the automotive industry where they are used for active suspension and skid control. These sensors range in cost from $25 to $1000 and are expected to drop in price in the future.

In this study the rate gyro that was used and tested extensively was the Systron Donner Horizon. The approximate price for these gyros is $700 for a single unit, $300 for 10-500 units, and $70 if purchased at rate of at least 3000 a year. The information provided on the manufacturer supplied data sheets are not normally sufficient for developing a good error model. Using methodology similar to that outlined in [6], error models for these gyros were developed.

Long Term Bias Stability

Characterization of the long term stability of the Horizon rate gyro was accomplished by constructing and analyzing an Allan-variance chart. Figure 1 shows an Allan-variance chart for one Systron Donner Horizon rate gyro. This chart is representative of all the other Systron Horizon rate gyros tested. The Allan variance for these gyros shows that for roughly the first 300 sec, the output error is dominated by wide band noise. Therefore, if the rate output from these gyros is integrated to give angle, the primary error would be angle random walk in this time period. Thus, for at least the first 300 sec filtering will minimize the error in the output. However, the gyros exhibit a long term instability which tends to dominate the output error after about 300 sec. The initial upward slope of approximately +1/2 indicates that the output error in that time period is predominately driven by an exponentially correlated process with a time constant much larger than 300 sec or a rate random walk.

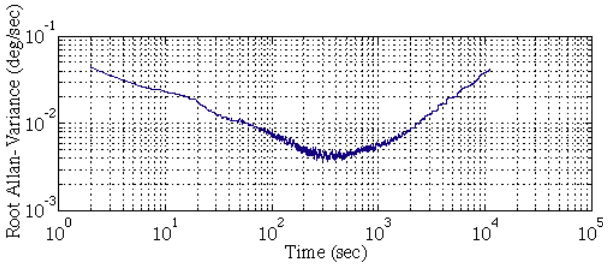

Figure 1. Allan Variance of Horizon

Scale Factor Tests

The gyros were placed on a single axis rate table that was installed in a temperature chamber. The rate table was rotated at an angular rate of 5 deg/sec while the output from the gyros was monitored. From this data the actual scale factor for the gyros was computed. This was repeated for a number of temperatures between 0 C and 60 C. From these tests it was concluded that the effect of temperature on scale factor is minimal (i.e., less than 2.6% change over the 0 C and 60 C range) and, therefore, excluded from the error model. Figure 2 shows the scale factor sensitivity to temperature of one of the rate gyros tested.

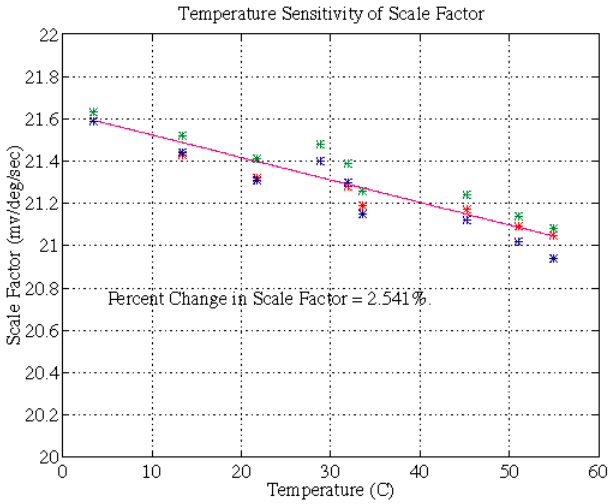

Figure 2. Temperature Sensitivity of Scale factor

Sensitivity of Bias to Linear Acceleration

The rate gyros were placed on a test bench in various orientations such that the internal vibrating element was subjected to accelerations between 0 and 1 g. The output of the rate gyros was monitored in these various orientations. From these tests it was concluded that the effect of linear acceleration, if any, was less than the gyro output noise and, therefore, excluded from the error model.

Effect of Temperature on Short-Term Bias Stability

The gyros were placed in a temperature chamber and the gyro output voltage was monitored. Since the rate gyros were not rotating, slow changes, if any, in the output voltage would be indicative of bias drift. This was repeated for a number of temperatures between 0 C and 60 C. The gyros were allowed to reach thermal equilibrium at each new temperature before data collection. Figure 3 shows the the output from three gyros that were used during this test. From these tests it was concluded that a *short term* (15 min) temperature effect was not observable and, as such, was not specifically accounted for in the error model. Based on the above testing and analysis, the error model used to describe the gyro bias instability was a random walk.

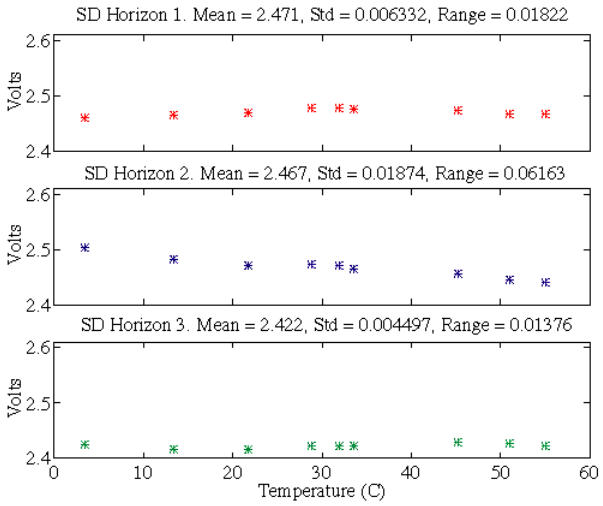

FIgure 3. Temperature Effect on Short Term Bias Stability

It is interesting to compare the long term stability of the Horizon gyros with that of other automotive grade gyros based on a different technology. Figure 4 shows an Allan-variance for an Andrew Autogyro. This is a Fiber Optic Gyro (FOG) which sells for approximately $900 per unit. Figure 4 shows that the long term stability of this gyro is substantially better than that of the Horizon. Asimilar modeling process for the FOG Andrew Autogyro resulted in a model for the bias which was a random constant corrupted by white sampling noise.

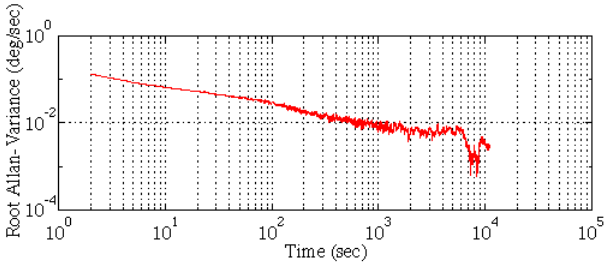

Figure 4. Allan-Variance for Andrew Autogyro

III. GPS ATTITUDE DETERMINATION

General

To take full advantage of the integration of inexpensive inertial sensors, it is important that the GPS attitude solution not contain any bias errors with time constants longer than the time constants of the gyros' bias instability. In order to achieve this requirement, two areas must be addressed. The first area is the choice of algorithm. Depending on which algorithm is used, given errors in phase measurements will result in different magnitudes of errors in the computed attitude. The second area to be addressed is the error characteristics of the L1 carrier phase measurements. These phase errors are a function of the receiver, the mounting of the antennas and the characteristics of the antennas.

The GPS attitude determination system used in this research consisted of a three antenna common clock GPS receiver. The three GPS antennas are oriented in an isosceles triangle with 36 cm and 50 cm legs. This configuration is small enough to be installed on top of the fuselage of a high or low wing GAaircraft. The small size allows for robust integrity monitoring due to the reduced integer resolution requirements, which is discussed in detail in [7].

Algorithm Selection

Two types of attitude algorithms have historically [8] been used: a known line/clock bias and an unknown line/clock bias. The unknown bias method solves for the bias at every epoch and as such does not require a common clock between all receiver-antenna pairs. This algorithm is used by attitude systems using multiple OEM boards with separate clocks. The known bias technique requires a common clock for all antennas and presumes a constant known line bias.

For each algorithm, a relationship can be made between baseline length and pointing accuracy for a given level of GPS phase error. This relationship is based on the concept of dilution of precision (DOP), discussed in depth in [7]. The case of L1 phase noise of 5 mm while tracking 6 satellites is shown in Figure 5 for the known bias and unknown bias algorithms.

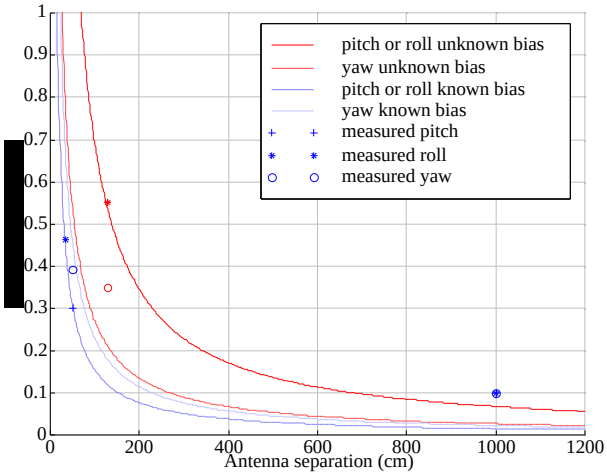

Figure 5. Angle errors vs. baseline length for different algorithms

The biggest difference between the two algorithms occurs in the pitch and roll directions. These are the most important parameters for displaying attitude. For a typical accuracy of .25 deg in pitch or roll there is more than a factor of four increase in antenna separation

required for the unknown bias case over the known bias case. Based on the limited space available on GAaircraft, the known bias algorithm with a common clock receiver is used in this implementation.

GPS Attitude Error Sources

Once the attitude algorithm has been optimized additional improvements in the attitude solution can be made be improving the quality of the differential phase measurements. The high frequency noise in the phase measurements may be averaged out by the inertial instruments but longer term errors must be calibrated out.

Long term phase errors can be broken down to those caused by multipath (i.e. signal reflection) and those caused by variation in antenna phase patterns. Phase delay maps for patch antennas are discusses extensively in [9]. By taking a single phase difference between two antennas, one effectively introduces any differences in the antenna phase delay patterns as phase errors. Both multipath and antenna phase errors have the effect of delaying the phase measurement as a function of the line of sight (LOS) vector from the antenna to the GPS satellites. In aircraft installations, the primary effect is from antenna phase error, as most multipath disappears when the aircraft is airborne. Indeed, the only multipath remaining on an aircraft in flight is due to the aircraft structure. This effect can be calibrated out in the same manner as the antenna phase error.

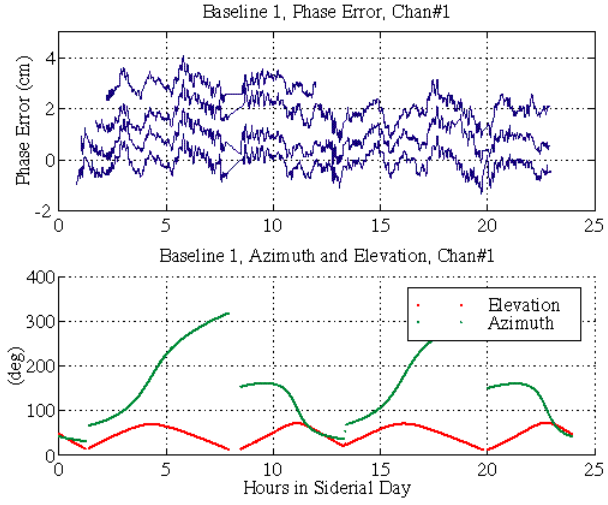

Figure 6. Plot of repeatability of GPS error

Figure 6 shows the repeatability of antenna phase errors for 4 days. The phase data shown is for one satellite taken at 2 Hz and averaged over 100 seconds. The 4 phase error lines were purposely offset by 1 cm increments every 24 hours for clarity.

It is important to notice the repeatability of even the very fine structure of the phase error as the satellite tracks through the same azimuth and elevation path. This implies that this error is deterministic and hence can be calibrated out. In addition, the very steep gradients of the phase error means that a very small change in LOS may cause a relatively large change in phase error. This necessitates a very fine grid when modeling the phase error over the full range of azimuth and elevation angles. However this extreme sensitivity of the error also means that a very small change in the attitude of the platform will cause the phase errors to de-correlate in time. Actual flight conditions are not perfectly static and effectively introduce dither. This dither effect changes the temporal characteristics of the phase error to a much higher frequency and and allows some of it to be filtered out by low grade inertial sensors. This effect reduces the phase error calibration requirement in actual aircraft applications.

The irregular spacing between the phase error lines from day to day indicates a slowly varying line bias effect. This phase offset is identical from channel to channel over the same time period and represents an additional error source to be considered later.

Figure 7. Top View of GPS Attitude Platform

In order to calibrate out this repeatable antenna phase error it is necessary to take phase measurements over all combinations of azimuth and elevation. Using the platform shown in Figure 7 it is possible to accomplish this by rotating the entire antenna array.

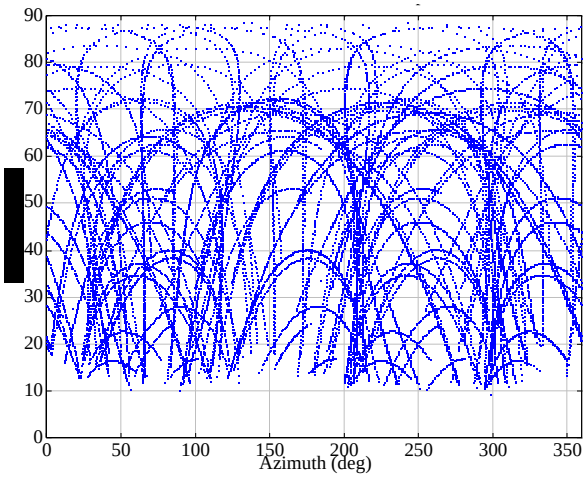

Figure 8. Line of Sight Relative to Platform Orientation

The LOS to the satellites relative to the platform is shown in Figure 8 for 3 different orientations over a total of 4 days. The maximum spacing between azimuth and elevation tracks is 4 degrees. Three orientations is the minimum number to adequately cover all azimuth and elevations. Ideally more orientations would be used to better cover the azimuth and elevation space.

These deterministic phase errors shown in Figure 6 have been modeled as a function of the relative azimuth and elevation of the satellite. The phase delay map for a given baseline is shown in Figure 9.

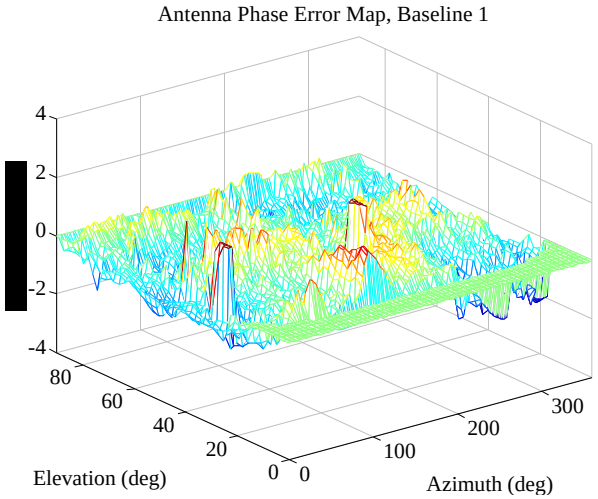

Figure 9. Plot of phase map for 1 baseline

There is as much as a 1 cm phase error introduced depending on the arrival azimuth and elevation angle to the satellite. As seen in Figure 10, by subtracting out the phase error from Figure 9, the rms error in the phase measurements decreases from 5 mm rms to 2.5 mm rms.

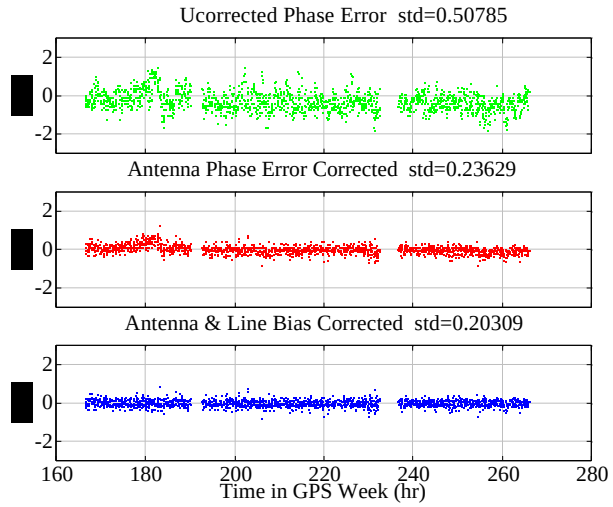

Figure 10. Phase error after antennae phase map removed

The second trace in Figure 10 shows an additional correlation with time. This is a change in line and clock biases that typically occurs as a result of temperature effects on the antenna cables. This error is common to all receiver channels for a given antenna pair and is slowly varying. If the error is averaged over a period of 4 hrs and then subtracted from the phase measurements the improvement is shown in the 3rd trace of Figure 10.

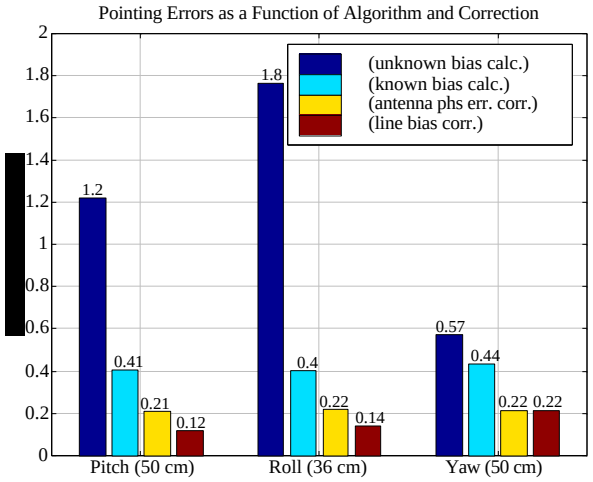

Figure 11. Summary of Pointing Error Improvements

The sequential improvements for pitch roll and yaw due to calibration of all error sources are shown in Figure 11 for a 6 channel receiver. The large gains in pitch and roll are obtained by using a common clock algorithm. Following that, improvements are made by calibrating out antenna phase error and changes in line biases. The final resulting performance is angular errors between 0.1° and 0.2° rms.

IV. FILTERING ALGORITHM

The attitude solution derived from the inertial sensors was blended with the attitude solution from the GPS triple antenna array using a constant gain filter. The algorithm used angular rates derived from the rate gyros at a rate of 20 Hz to propagate the attitude solution in time. The airplane attitude was parameterized in terms of euler angles. Euler angle parameterization allowed sending the attitude solution directly to the display at 20 Hz without increasing the computational burden on the microprocessor performing the computations. The state vector for this estimation process is defined as follows:

$$x = \begin{bmatrix} \psi & \theta & \phi & \delta p & \delta q & \delta r \end{bmatrix}^T \quad (1)$$

The first three entries in the state vector are the yaw, pitch and roll states respectively while the remaining three entries are the roll, pitch and yaw axis gyro biases respectively. The input vector in the estimator is:

$$u = \begin{bmatrix} p & q & r \end{bmatrix}^T \quad (2)$$

The entries in this vector are the roll, pitch and yaw axis gyro outputs respectively. The time update equation for

the state estimation is:

$$\dot{\hat{x}} = F\hat{x} + Gu \tag{3}$$

The F matrix is

$$F = \begin{bmatrix} 0_{(1\times1)} & f(\theta,\phi)_{(1\times1)} \\ 0_{(1\times1)} & 0_{(1\times1)} \end{bmatrix} \tag{4}$$

The submatrix f is given by

$$f(\theta,\phi) = \begin{bmatrix} 0 & \frac{\sin\phi}{\cos\theta} & \frac{\cos\phi}{\cos\theta} \\ 0 & \cos\phi & -\sin\phi \\ 1 & \sin\phi\tan\theta & \cos\phi\tan\theta \end{bmatrix} \tag{5}$$

The input matrix G is:

$$G = \begin{bmatrix} f(\theta,\phi)_{(1\times1)} \\ 0_{(1\times1)} \end{bmatrix} \tag{6}$$

The measurement equation (which is solved at 2 Hz) is given by:

$$\hat{x}^{(+)} = \hat{x}^{(-)} + L(y - H\hat{x}) \tag{7}$$

The measurement vector y is given as

$$y = \begin{bmatrix} \psi_{gps} & \theta_{gps} & \phi_{gps} \end{bmatrix} \tag{8}$$

The measurement matrix H is defined as:

$$H = \begin{bmatrix} I_{(1\times1)} & 0_{(1\times1)} \end{bmatrix} \tag{9}$$

The estimator gain matrix L is computed "off-line." The input to the algorithm that computes the estimator gain are the process and measurement noise matrices. The process noise covariance matrix was determined as part of the error model in Section II and the measurement noise covariance matrix is determined from the noise measurement from the output of the GPS attitude algorithm.

V. FLIGHT TEST RESULTS

The above algorithm was implemented a in real-time AHRS and flight tested on a Beechcraft Queen Air. The attitude information from the AHRS was displayed on

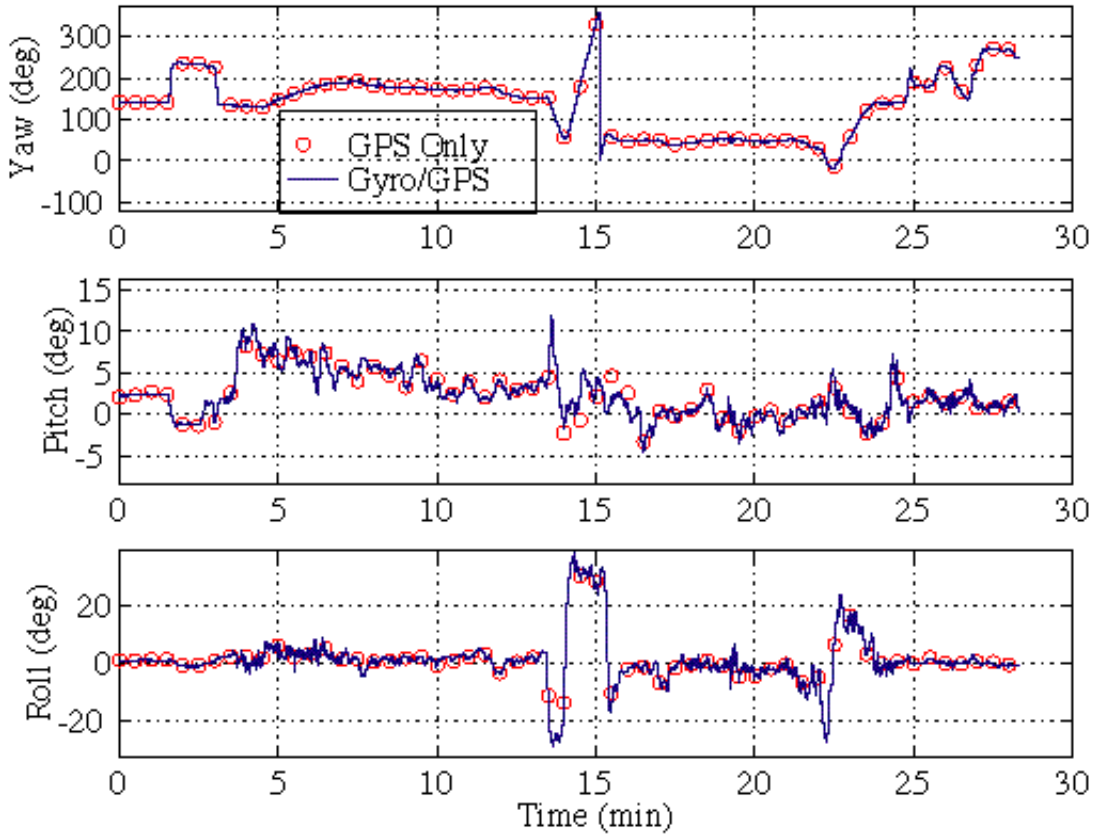

Figure 12. Attitude Time History (For plotting purposes, the 2 Hz raw GPS attitude solution is shown at 30 sec intervals).

a “glass-cockpit” display described in [10] and used for real-time pilot in the loop control of the aircraft. Throughout the flight test period the display was evaluated for latency and correlated with the other attitude reference instruments and the view of the horizon outside the window. The 20 Hz update rate was found to be sufficient to present a fluid display with no observable jitter or lag by the pilots. The time history plot shown in Figure 12 demonstrates this. A comparison of the raw GPS attitude solution with the integrated gyro solution shows no lag in the gyro smoothed attitude solution displayed.

The high bandwidth information from the gyros also eliminated jitter in the displayed attitude solution. Figure 13 shows the smoothing achieved by the gyros. Pilots who flew the Beech Queen Air test aircraft using the attitude information displayed by this system reported they had no difficulty controlling the aircraft using only the attitude information generated by the integrated GPS and gyro system.

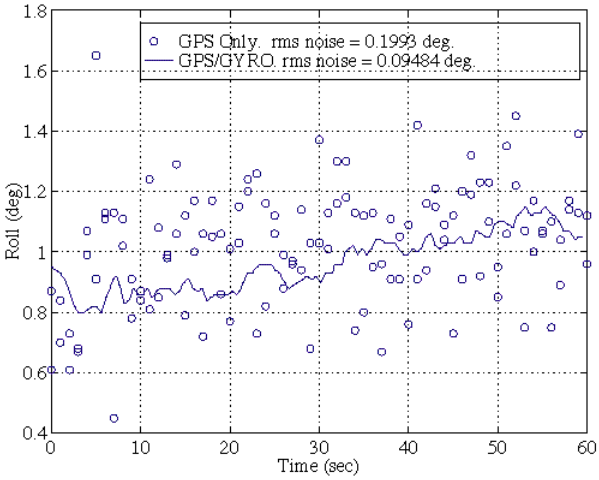

Figure 13. Filtering of GPS attitude Solution

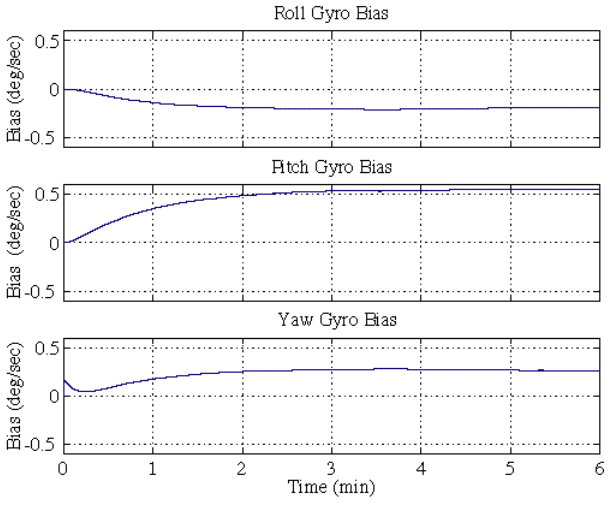

Figure 14. Gyro Bias Convergence

Figure 14 shows the convergence of the gyro biases. The estimates of gyro biases stabilized after about 4 minutes from power up. The estimation of gyro biases allows the system to accurately provide attitude information during temporary GPS outages.

As a demonstration of the coasting capability of the system, feedback from the GPS attitude solution was deliberately turned off in data post processing by setting the estimator gain L = 0 for an extended period of time. The plots in Figure 15 show the deviation between the gyro integrated attitude solution and the GPS attitude solution during this outage. There is less than a 4 degree error in all axes 5 minutes after the GPS feedback has been removed. Simulations using the error models developed in Section II show that in the worst case, attitude errors (1 sigma) can be expected to grow at a rate of 2.5 degrees per minute for a system using the Systron Donner Horizon rate gyros and at 0.5 degrees per minute for a system using the Andrew Autogyro [7].

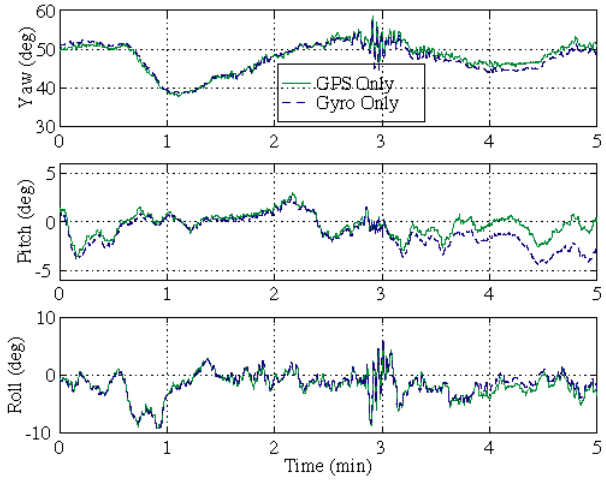

Figure 15. Gyro Coast Capability (GPS outage occurs at time t = 0).

Flight test experience has demonstrated that GPS outages in flight are rare and of a short duration. For example, during one of the recent series of flight tests, the AHRS operated for total of 2.5 hours of flight time during which the longest GPS outage lasted only six seconds. Most of the outages were of a shorter duration. The Systron Donner Horizon rate gyros can adequately coast through such outages; however, for protection against more extensive outages, a FOG would be desirable.

VI. SUMMARY AND CONCLUSION

In order to achieve sub-degree accuracies in pitch and roll for the ultra-short baseline attitude systems it was necessary to utilize the known bias algorithm with a common clock receiver. By mapping the inter-antenna

phase patterns, the phase error was reduced to 2.5 mm rms. More importantly, the slowly varying nature of the error was removed. This allows the inexpensive inertial instruments to be used effectively to filter out noise and provide higher bandwidth output.

Low cost automotive grade rate gyros adequately filter the high frequency noise in a short baseline GPS attitude system. This filtering enables the use of such an AHRS for pilot-in-the-loop control of general aviation aircraft. It has also been demonstrated that in-flight calibration of low cost inertial sensors can cause the sensors to perform at the level of low grade tactical inertial sensors for short periods of time. However, the long term coasting ability of such gyros is not a function of the use of on-line calibration by GPS but rather the stability of the inertial sensors. The low end automotive grade rate gyros used in the AHRS described in this paper did not have the stability required for long coasting times. The coast time of such an AHRS can be extended if Fiber Optic Gyros like the Andrew Autogyro are used.

VII. ACKNOWLEDGEMENTS

The authors gratefully acknowledge the many friends and colleagues at Stanford University who have helped us in this effort. In particular,Andrew Barrows for providing the display that allowed use of the AHRS in real-time control and Sharon Houck and Matthew Jardin who helped during flight tests. We also wish to thank Seagull Technology Inc. and NASA-Langley for the technology transfer grant that supported this work.

REFERENCES

[1] Da, Ren, “Investigation of a Low Cost and High-Accuracy GPS/IMU System”, Proceedings of the ION National Technical Meeting, Santa Monica, CA, January 1997.

[2] Wolf, R. et.al, “An Integrated Low Cost GPS/INS Attitude Determination System and Position Location System”, Proceeding of ION-GPS 96, Kansas City, Missouri, September 1996. pp. 975-981.

[3] Montgomery, P. Y., Carrier Differential GPS as a Sensor for Automatic Control, Ph.D Thesis, Stanford University, 1996.

[4] Archangel Avionics Inc., EFIS/EICAS and FMS brochure, 1997.

[5] Kornfeld, R.P., Hansman, R. J., Deyst, J. J., “Single Antenna GPS Based Aircraft Attitude Determination,” Proceedings of the Institute of Navigation National Technical Meeting, Long Beach, CA, Jan. 1998.

[6] IEEE Std 647-1995, “IEEE Standard Specification Format Guide and Test Procedures for Single Axis Laser Gyros,” May 1996.

[7] Hayward, R.C. et. al., “Inertially Aided GPS Based Attitude Heading Reference System (AHRS) for General Aviation Aircraft”, Proceedings of ION-GPS-97, Kansas City, MO, Sep. 1997, pp. 289-298.

[8] Euler, H. J., and Hill, C. H., “Attitude Determination: Exploring all Information for Optimal Ambiguity Resolution”, Proceedings of the ION GPS-95, Palm Springs, CA, Sept. 1995, pp 1751-1757.

[9] Tranquilla, James M. and Colpitts, Bruce G., “GPS Antenna Design Characteristics for High-Precision Applications”, Journal of Surveying Engineering, Vol. 115, No. 1, February, 1989

[10] Barrows et. al. “Flying Curved Approaches: 3-D Display Trials Onboard Light Aircraft”, Proceedings of the 9th International Technology Meeting of the Satellite Division of the ION-97, Sep 17-20, Kansas City MO, p 59-68.